



SPECT Imaging of Acute Disc Herniation by Targeting Integrin $\alpha 5\beta 1$ in Rat Models

Jian Guan^{1,2,3,4†}, Chenghua Yuan^{1,2,3,4†}, Xin Tian⁵, Lei Cheng^{1,2,3,4}, Hannan Gao⁶, Qingyu Yao^{1,2,3,4}, Xinyu Wang^{1,2,3,4}, Hao Wu^{1,2,3,4}, Zan Chen^{1,2,3,4*} and Fengzeng Jian^{1,2,3,4*}

¹ Department of Neurosurgery, Xuanwu Hospital, Capital Medical University, Beijing, China, ² Spine Center, China International Neuroscience Institute (CHINA-INI), Beijing, China, ³ Research Center of Spine and Spinal Cord, Beijing Institute of Brain Disorders, Capital Medical University, Beijing, China, ⁴ National Center for Neurological Disorders, Xuanwu Hospital, Beijing, China, ⁵ Center for Experimental Animals, Xuanwu Hospital, Capital Medical University, Beijing, China, ⁶ Medical Isotopes Research Center and Department of Radiation Medicine, State Key Laboratory of Natural and Biomimetic Drugs, School of Basic Medical Sciences, Peking University, Beijing, China

OPEN ACCESS

Edited by:

Volker Rasche,
University of Ulm, Germany

Reviewed by:

Zohar Keidar,
Rambam Health Care Campus, Israel
Simona Ben-Haim,
Hadassah-Hebrew University Medical
Center, Israel

*Correspondence:

Zan Chen
chenzan66@163.com
Fengzeng Jian
jianfengzeng@xwh.ccmu.edu.cn

†These authors have contributed
equally to this work

Specialty section:

This article was submitted to
Applied Neuroimaging,
a section of the journal
Frontiers in Neurology

Received: 20 November 2021

Accepted: 14 March 2022

Published: 09 May 2022

Citation:

Guan J, Yuan C, Tian X, Cheng L,
Gao H, Yao Q, Wang X, Wu H, Chen Z
and Jian F (2022) SPECT Imaging of
Acute Disc Herniation by Targeting
Integrin $\alpha 5\beta 1$ in Rat Models.
Front. Neurol. 13:782967.
doi: 10.3389/fneur.2022.782967

Objective: Traditional morphological imaging of intervertebral disc herniation (IVDH) is challenging in early disease diagnosis. Aiming at the early diagnosis of IVD by non-invasive molecular imaging targeting of integrin $\alpha 5\beta 1$, we performed novel imaging in rats with acute IVDH for the first time.

Methods: Animal models were prepared by conducting an established needle puncture procedure through the normal intervertebral disc (IVD). The disc-injured rats underwent SPECT/CT imaging of the ^{99m}Tc-3PisoDGR2 peptide at 1 day to 2 months postinjury. The expression change of integrin $\alpha 5\beta 1$ was determined by anti-integrin $\alpha 5$ and anti-integrin $\alpha 5\beta 1$ immunohistochemistry (IHC). Magnetic resonance imaging (MRI) was performed for comparison during disease progression. The morphological changes of the disc were determined by safranin-O staining.

Results: Rats with acute IVDH showed gradually increased disc uptake of ^{99m}Tc-3PisoDGR2 from 1 to 7 days posttreatment, which was a significantly higher level than that of the normal disks in degenerative diseases. IHC results showed the expression of integrin $\alpha 5\beta 1$ on the surface of annulus fibrosus (AF) cells and nucleus pulposus (NP) cells, which agreed with the uptake data. MRI showed a progressively decreased T2 density and MRI index throughout the investigation. Hematoxylin and eosin (HE) staining and safranin-O staining revealed a disorganized structure of the IVD as well as loss of proteoglycans after puncture.

Conclusions: The present study demonstrated a good correlation between integrin $\alpha 5\beta 1$ expression and acute disc herniation. The SPECT/CT imaging of ^{99m}Tc-3PisoDGR2 targeting integrin $\alpha 5\beta 1$ may diagnose IVDH in an acute phase for early disease management.

Keywords: molecular imaging, integrin $\alpha 5\beta 1$, ^{99m}Tc-3PisoDGR2, disc herniation, acute

INTRODUCTION

Lumbar disc herniation, a common disease that causes low back pain (LBP) (1), is a worldwide issue leading to human incapacity (2). To avoid irreversible degenerative disc herniation, early diagnosis of intervertebral disc (IVD) pathological changes is crucial for disease management in quinquagenarians who are at high risk (3, 4). Although traditional computed tomography (CT) and magnetic resonance imaging (MRI) are the most common noninvasive strategies for the diagnosis of lumbar disc diseases (5), advice based on morphological changes at the early stages of disc herniation remains elusive (6). Compared to anatomical imaging, molecular imaging provides precise and specific information for detecting disease in the early stage.

Strategies for the molecular diagnosis of disc herniation by certain biomarkers are of interest (7). Unlike most normal tissues with high contents of blood vessels and nerves, the nucleus pulposus (NP) in the IVD possesses a high content of matrix cells and extracellular matrix (8, 9). Fibronectin, a classical extracellular matrix component, is highly expressed by local disc cells during disc degeneration (10), and its receptor, integrin $\alpha 5\beta 1$, plays an important role in regulating inflammatory cytokines produced by human articular chondrocytes (11). Therefore, integrin $\alpha 5\beta 1$ may be a biomarker for the early diagnosis of disc herniation. However, traditional immunohistochemistry (IHC) tests by invasive biopsies or surgery are not practical in spines, but molecular imaging can assess receptor expression in a real-time and non-invasive manner (12, 13). Moreover, peptide imaging probes show rapid clearance from circulation, good tissue penetration, and high specificity for real-time imaging (14).

Recently, molecular imaging targeting of integrin $\alpha 5\beta 1$ by single-photon emission computed tomography (SPECT) or positron emission tomography (PET) imaging has been investigated for tumor and rheumatoid arthritis diagnosis (15–17). However, molecular imaging targeting of integrin $\alpha 5\beta 1$ in disc herniation has not been reported. Recently, we reported a radiolabelled isoDGR dimer peptide of ^{99m}Tc -3PisoDGR₂ for SPECT/CT imaging to diagnose integrin $\alpha 5\beta 1$ -positive tumors (18). In the present study, we hypothesized that high integrin $\alpha 5\beta 1$ expression in intervertebral disks indicates pathological changes at the molecular level for detecting early lumbar disc herniation. Therefore, we applied SPECT/CT imaging of ^{99m}Tc -3PisoDGR₂ in acute disc herniation rat models. In contrast to traditional MRI, this imaging strategy showed evident advantages in the early diagnosis of disc herniation.

MATERIALS AND METHODS

Animals

A total of 26 male Sprague-Dawley rats (12 weeks old; 250–300 g) were purchased from the Experimental Animal Research Center, Chinese Academy of Medical Science, Beijing, China. The rats were housed in standard sterile pathogen-free facilities (temperature, $20 \pm 2^\circ\text{C}$; humidity, 50–60%; and 12-h light/dark cycle) and given free access to food and water. In the experimental group (14 rats in total), five rats were evaluated

by imaging, and samples from the other nine rats were collected for histology at different time points after the operation. In the control group (12 rats in total), three rats were evaluated by imaging, and samples from the other nine rats were collected for histology at different time points after the operation. The present study was approved by the Institutional Review Board (XWH20200206), and the animal care complied with the Guide for the Care and Use of Laboratory Animals.

Study Design

The experimental flowchart is presented in **Figure 1**. The grouping information and number of rats at each checkpoint are listed in **Table 1**.

Surgical Procedure

Rats were anesthetized by inhaling isoflurane gas (2% enflurane in 70% nitrous oxide and 30% oxygen), and the surgery was performed according to the routine procedures (19). Briefly, after palpation to locate the caudal levels, a needle (18-gauge with an outer diameter of 0.84 mm) was inserted into the middle part of the NP at Co5/6 and Co6/7 while being guided by C-arm X-ray (GE Brivo OEC850, GE Company, Boston, USA). The needle was rotated 180° and held for 5 s. The depth of penetration was controlled by locking forceps (clamped 5 mm from the tip of the needle). We just put the needle into the skin, and the NP of Co4/5 and Co7/8 remained undisturbed as the control reference.

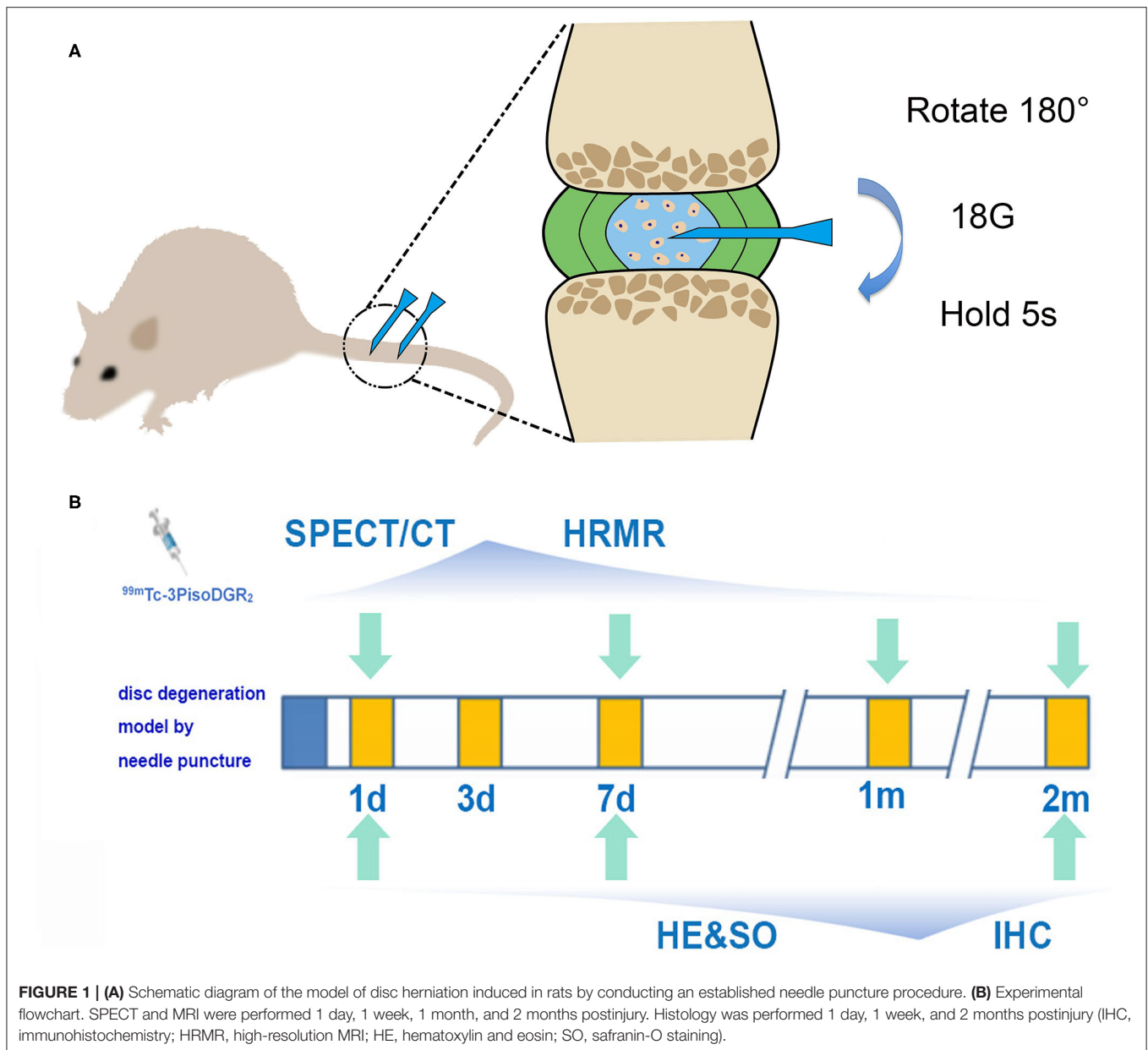
Magnetic Resonance Imaging Measurements

Magnetic resonance imaging was performed 1 day, 1 week, 1 month, and 2 months postoperatively (7.0-T MRI scanner, Bruker, Germany, interfaced with Siemens software). Briefly, after inhaling anesthesia, the animal was laid prone, and the tail was straightened in a double-tuned volume radiofrequency coil. Eight serial T2-weighted sagittal images covering the entire disc area were acquired using a spin-echo sequence. The T2WI sequence parameters were as follows: fat saturation, on; repetition time/effective echo time, 3,000/30 ms; field of view, 30 mm \times 60 mm; matrix, 128 \times 128; slice thickness, 0.5 mm; slice spacing, 0 mm; number of slices, 8; and number of scans, 1 (total scan time = 6.24 min) (7).

Quantitative analysis of the obtained image slices was performed using Analyze 7.0 (AnalyzeDirect). The nucleus region was segmented from the sliced images. Image reconstruction and volume rendering procedures were performed to generate volumetric images and to calculate each nuclear volume. T2-weighted density and MRI index (the area of NP \times average signal intensity) were quantified and calculated (7). All image assessments were conducted by three observers independently who were blinded to the study grouping.

SPECT/CT Imaging

In this study, we used two SPECT probes that target different integrins. The integrin $\alpha 5\beta 1$ -targeted ^{99m}Tc -3PisoDGR₂ was prepared according to our previous studies (15, 18, 20). To



prepare ^{99m}Tc -3PisoDGR₂, a mixture of 20 μg of HYNIC-3PisoDGR₂, 6 mg of TPPTS (J&K Chemical Ltd., Beijing, China), 5 mg of tricine, and 74 MBq $\text{Na}^{99m}\text{TcO}_4$ was reacted in 50 mM succinate buffer (pH = 5.0) at 99°C for 15 min. The radiochemical purity (RCP) was determined by radioactive reverse-phase high-performance liquid chromatography (RP-HPLC), resulting in 95% RCP before *in vivo* applications. The integrin $\alpha\beta 3$ -targeted ^{99m}Tc -3PRGD₂ peptide was prepared according to the literature (21), resulting in 95% RCP before *in vivo* applications.

To explore the integrin expression level changes during the progress of acute disc herniation disease, rats were undergoing ^{99m}Tc -3PisoDGR₂ or ^{99m}Tc -3PRGD₂ SPECT/CT imaging at 1 day, 1 week, 1 month, and 2 months. Rats were anesthetized with

2% isoflurane, a surgical incision was made in the inner thigh, and vena femoralis injection for 74 MBq ^{99m}Tc -3PisoDGR₂ or ^{99m}Tc -3PRGD₂, suturing was performed after injection. SPECT/CT imaging was using a Nano SPECT/CT imaging system (Mediso Ltd., Hungary). SPECT/CT imaging was performed at 0.5-h post-injection. SPECT was performed using four parallel aperture collimators (peak: 140 keV, 20% width; frame time of 20 s), and CT was performed using a helical scan (50 kVp; exposure time of 300 ms). The SPECT and CT images were merged using Nucline software v2.0 (Mediso Ltd.). The SPECT/CT data were analyzed using ASIPro software (version 3.2). The SPECT quantification was determined by ratios of probe uptake (T/NT) of the injured IVD to the adjacent normal intervertebral disc.

TABLE 1 | Grouping information ($N = 26$ in total).

	No. of rats at each checkpoint								In total
	Post-op 1-day		Post-op 1-week		Post-op 1-month		Post-op 2-month		
	Group 1 injury	Group 2 sham	Group 1 injury	Group 2 sham	Group 1 injury	Group 2 sham	Group 1 injury	Group 2 sham	
MRI and SPECT ^a	5	3	5	3	5	3	5	3	8
Histology ^b	3	3	3	3	N/A	N/A	3	3	18

^aFive rats and three rats were assigned to injury group and sham group, respectively. SPECT/CT imaging was performed one day after each MRI time point.

^bThree rats from each group were sacrificed at each checkpoint.

MRI, Magnetic Resonance Imaging; SPECT, Single Photon Emission Computed Tomography.

Histology

The number of sacrificed rats for each time point is shown in **Table 1**. Coccygeal spinal columns were dissected, postfixed in 10% paraformaldehyde overnight, and decalcified with 0.25 M ethylenediaminetetraacetic acid (EDTA) for 3 days. The specimens were embedded in paraffin wax blocks. Median sagittal 5- μ m sections were cut with a microtome and mounted on glass slides. The sections were air-dried for at least 4 h before staining. Sections were stained with hematoxylin and eosin (HE) and 0.1% Safranin-O to confirm the degenerative changes in the IVD after needle puncture, including the changes in morphological structure and proteoglycan expression.

Immunohistochemistry

Immunohistochemistry was performed to determine the presence of protein and the localization of integrins $\alpha 5$ and $\beta 1$. Sections were incubated with diluted rabbit polyclonal anti-integrin $\alpha 5$ antibody (1:100; Santa Cruz Biotechnology) or diluted rabbit monoclonal anti-integrin $\beta 1$ antibody (1:100; Epitomics) at 4°C overnight. The signal was visualized with 3,3'-diaminobenzidine (DAB). The sections were imaged using an image analysis system (Leica TCS SP2, Leica, Wetzlar, Germany). Immunoreactive cells were quantified by calculating the average value of three slides (8 μ m thick and 80 μ m interval) using ImagePro Plus software. The number of $\alpha 5$ -positive and $\beta 1$ -positive cells in the studied regions was counted with a $\times 40$ objective. Three distinct field-of-views were randomly selected for counting from anterior edges adjacent to the punctured annulus.

Statistical Analysis

All data are presented as the mean \pm standard deviation (SD). SPSS 22.0 (IBM SPSS, Armonk, NY, USA) was used for statistical analysis. Radioactivity of the disc injury region *in vivo* and MRI data were analyzed by repeated-measures ANOVA with Tukey's multiple comparisons test. Statistical analysis for IHC was performed using one-way ANOVA with Tukey's multiple comparisons test. The $p < 0.05$ was considered statistically significant. Origin 8.5 (Northampton, MA, USA) was used to generate the graphs.

RESULTS

In vivo Imaging of Integrin $\alpha 5\beta 1$ Expression by Non-invasive SPECT

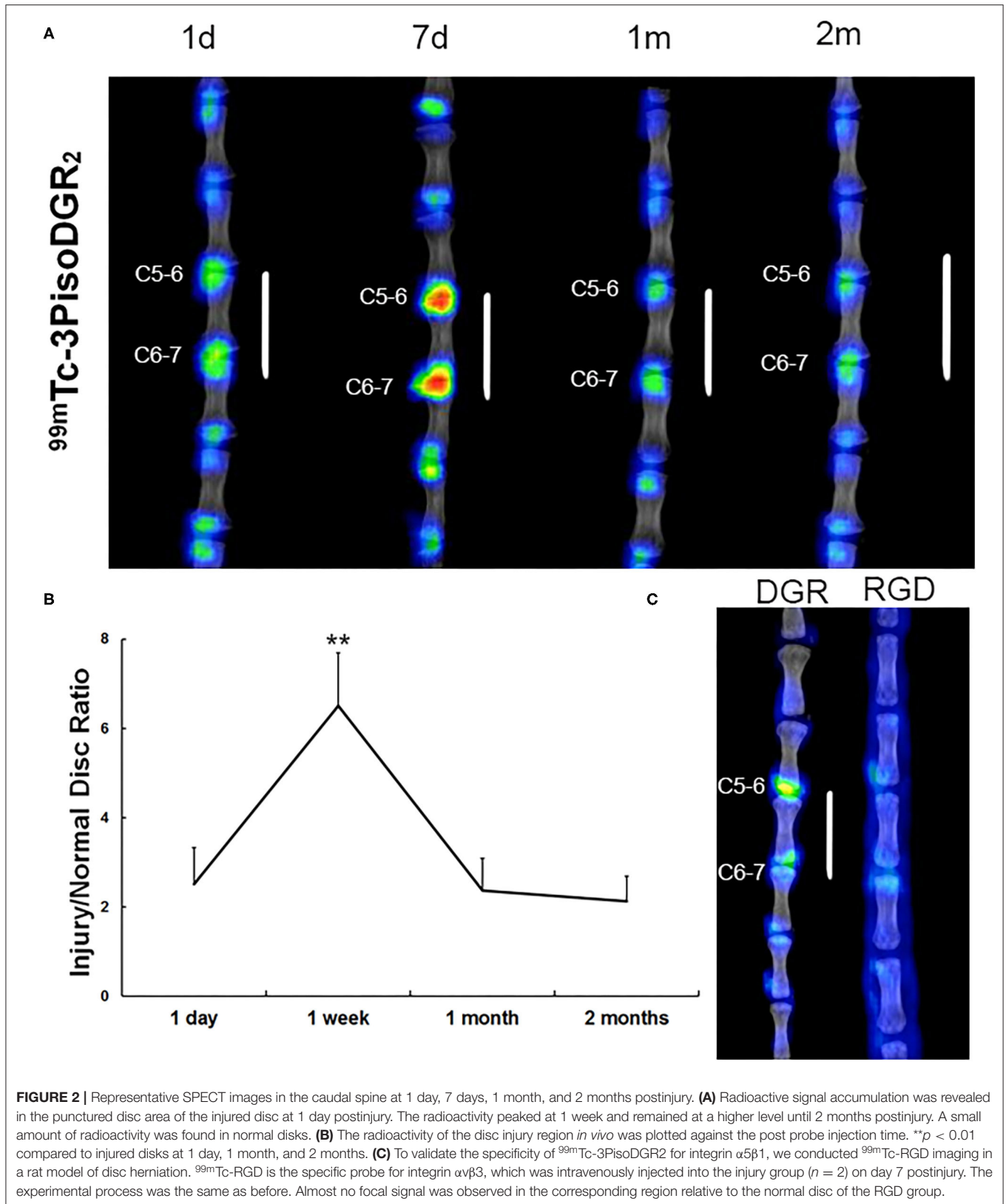
Compared to normal IVD, the expression of integrin $\alpha 5\beta 1$ was significantly upregulated in the NP of injured IVD at each time point (**Figures 2A,B**). The radioactivity significantly accumulated in the punctured disc at 1 day postinjury, reached a peak at 1 week postinjury ($p < 0.01$), and gradually decreased from 1 month postinjury (**Figures 2A,B**). No focal signal was observed in the corresponding disc region of the RGD group (the specific probe for integrin $\alpha v\beta 3$) at 7 days postinjury, whereas nonspecific diffusion imaging was observed on the skin and subcutaneous tissue (**Figure 2C**). These results demonstrated that ^{99m}Tc-3PisoDGR2 has high specificity for integrin $\alpha 5\beta 1$.

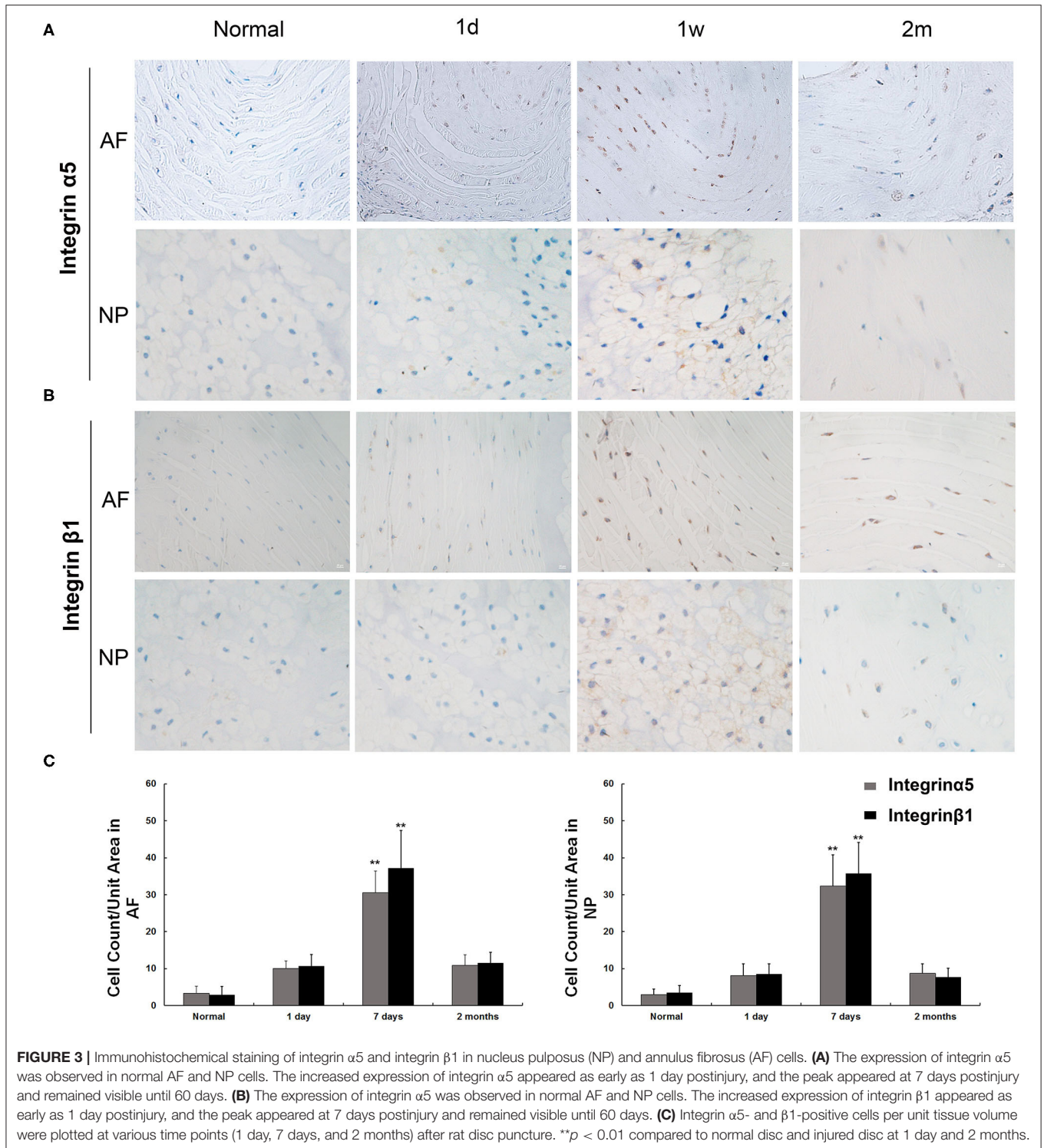
Ex vivo Confirmation of Integrin $\alpha 5\beta 1$ Expression by IHC

The IHC staining showed that integrin $\alpha 5$ and integrin $\beta 1$ were expressed on the surface of NP and annulus fibrosus (AF) cells in the control group (**Figures 3A,B**). In the injured group, the expression levels of integrin $\alpha 5$ and integrin $\beta 1$ were slightly increased at postoperative day 1. One week after injury, extensive-expression of integrin $\alpha 5$ and $\beta 1$ was observed on the membranes of NP and AF cells ($p < 0.01$). Two months after the injury, the distribution of NP and AF cells was scattered in the IVD, and the IHC staining on the cell surface was uneven. Moreover, the expression levels of integrin $\alpha 5$ and $\beta 1$ at 2 months postinjury were decreased but were still higher than those in the control group (**Figure 3**). The changing pattern of *ex vivo* expression of integrin $\alpha 5\beta 1$ was consistent with that of *in vivo* detection by SPECT/CT.

In vivo Evaluation of Morphological Changes by MRI

T2-weighted midsagittal MRI of the caudal disks in a representative case is shown in **Figure 4A**. At 1 day postinjury, the T2 density was high on the NP and low on the endplate. The adjacent vertebrae were separated, and the height of the intervertebral space was normal. The T2 density continued to increase until 1 week postinjury and then began to decrease after 1 month postinjury. Finally, T2 density reached the lowest with

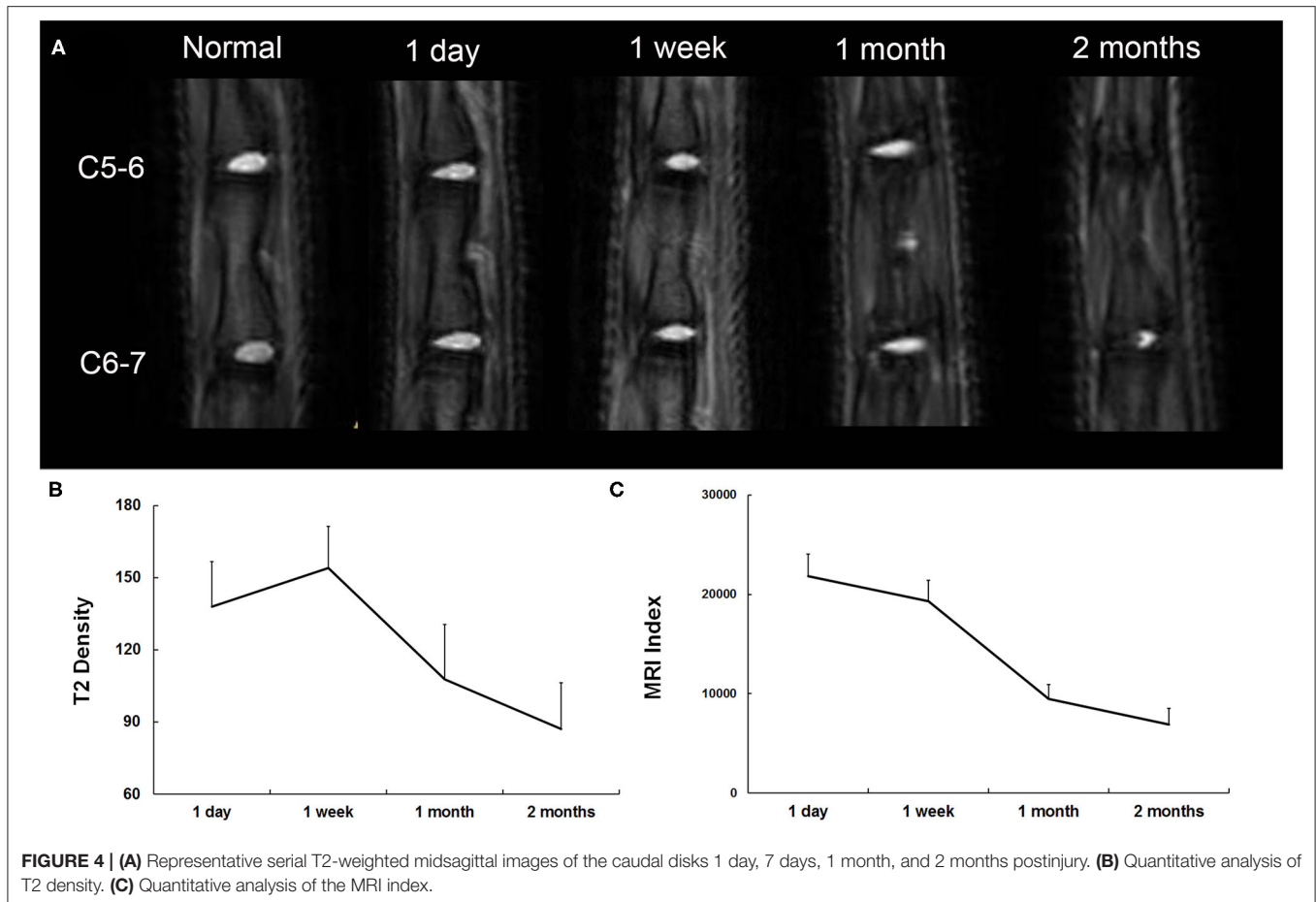




narrowed intervertebral space at 2 months postinjury. The MRI index significantly decreased from 1 week to 2 months postinjury (Figure 4). In contrast to T2 density, the changing pattern of the MRI index was a monotone decreasing curve at each time point (Figure 4C).

Ex vivo Confirmation of Morphological Changes by Histological Staining

The border between the AF and the NP was determined by HE staining at postoperative day 1 (Figure 5A). However, at 1 week postinjury, the number of notochordal cells and chondrocyte-like



cells in the NP began to decrease, and the arrangement of the AF began to become disordered with a blurred border. At 1 month postinjury, the number of notochordal cells and chondrocyte-like cells in the NP was further reduced, and fibroblast-like cells and degenerative necrotic cells emerged. At 2 months postinjury, the NP had almost disappeared and was replaced by fibrocartilage tissue, whereas the arrangement of AF was still disordered with a blurred border. The same changing pattern was also observed with safranin-O staining, indicating decreased proteoglycan (**Figure 5B**).

DISCUSSION

Low back pain, a pivotal factor leading to the decline or even loss of the workforce, is a common clinical symptom in modern society that places larger physical, psychological, and economic burdens on patients and their families (22). Owing to the accelerated aging of the population, the number of patients suffering from LBP has continued to increase (23). Disc herniation is acknowledged as one of the most common causes of LBP (24). Occupational epidemiology studies have shown that traumatic injury, heavy physical work, lifting, and excessive straining are important risk factors for disc herniation (25).

The IVD is composed of the upper cartilage endplate, lower cartilage endplate, AF and NP. A normal NP in the IVD has a high matrix content but few blood vessels and nerves. These physiological characteristics suggest that the interplay between IVD cells and the extracellular matrix substantially influences degeneration. Integrins are a class of transmembrane proteins that are widely distributed on the cell surface, connecting cells with the extracellular matrix to maintain the structural and mechanical integrity of the cell. Moreover, integrins transmit mechanical signals and biochemical signals of the extracellular matrix into the cell and are involved in several biological functions, such as cell survival, apoptosis, and gene expression (26, 27). Integrin $\alpha 5\beta 1$ is a classic fibronectin receptor that is mainly expressed in the chondrocytes of adults (28). By linking fibronectin fragments in chondrocytes, integrin $\alpha 5\beta 1$ initiates the downstream cascade signal amplification effect, thereby leading to matrix degradation and remodeling (29). IVD NP cells are similar to articular cartilage cells in terms of tissue origin and composition, and recent studies have shown that such a pathway exists in IVDs (30, 31). Therefore, it is postulated that integrin $\alpha 5\beta 1$ is an important cell membrane receptor for IVD degeneration.

The changes in integrin $\alpha 5\beta 1$ on the surface of IVD cells during disc degeneration remain controversial (32, 33).

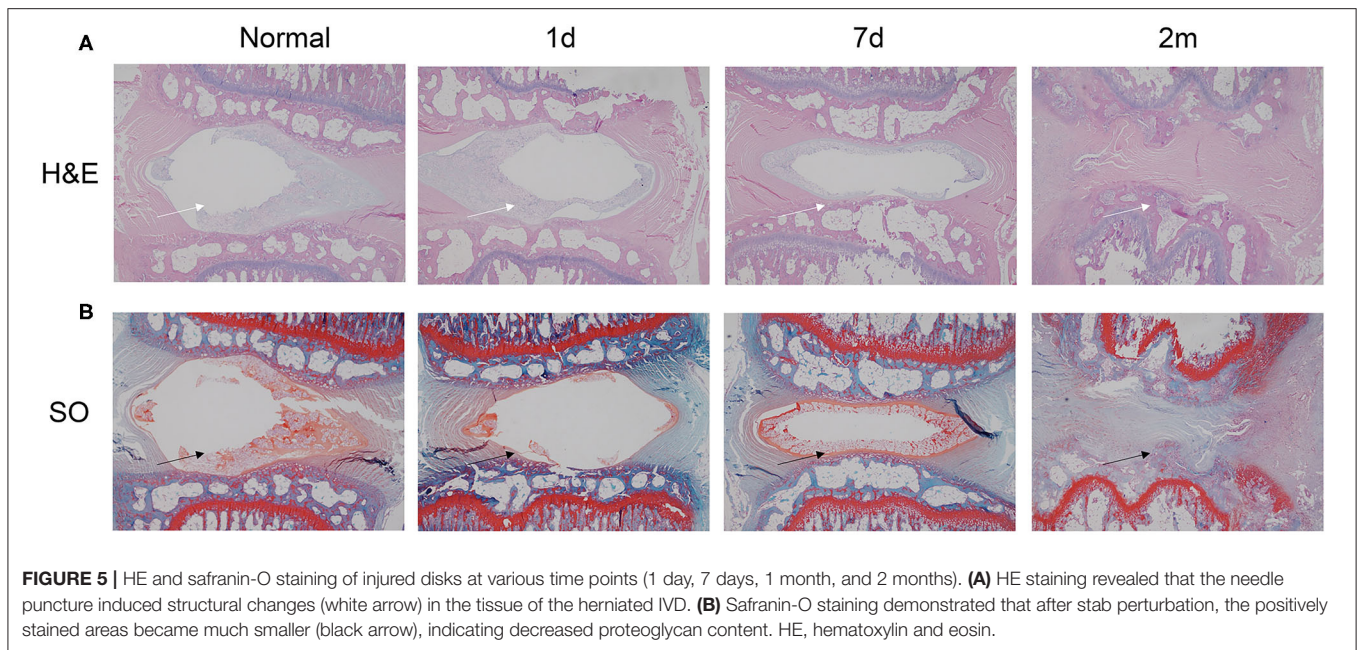


FIGURE 5 | HE and safranin-O staining of injured disks at various time points (1 day, 7 days, 1 month, and 2 months). **(A)** HE staining revealed that the needle puncture induced structural changes (white arrow) in the tissue of the herniated IVD. **(B)** Safranin-O staining demonstrated that after stab perturbation, the positively stained areas became much smaller (black arrow), indicating decreased proteoglycan content. HE, hematoxylin and eosin.

Kurakawa et al. (32) found that under pressure, the high expression of integrin $\alpha 5\beta 1$ in NP and AF cells is involved in the process of disc degeneration. However, Zhang et al. (34) found that under unbalanced dynamic and static forces, the expression of integrin $\alpha 5\beta 1$ in disc cells decreases, subsequently inducing excessive apoptosis of disc cells. Christine et al. (30) performed IHC on NP cells from normal and degenerated human disks and found that the expression level of integrin $\alpha 5\beta 1$ does not significantly change during disc degeneration. Such inconsistent results may be attributed to different time points and different modeling methods of IVD degeneration. An in-depth understanding of how integrin $\alpha 5\beta 1$ is involved in disc degeneration, thereby leading to excessive apoptosis of disc cells and matrix degradation, will be helpful to shed light on the pathophysiologic progression of disc degeneration.

However, a sensitive, non-invasive, and efficient method has not been developed for the detection of integrin $\alpha 5\beta 1$ in IVD. The traditional detection methods mainly include reverse transcription-polymerase chain reaction (RT-PCR), Western blotting, and IHC staining, which are impracticable for observing real-time changes in expression in the same individual *in vivo*. Current imaging diagnostic techniques to assess the degree of disc degeneration, such as X-rays and MRI, are conducted based on morphological aberrations. Molecular imaging technology can target molecules or biological macromolecules *in vivo* to reflect specific cellular and molecular events (35). Previous studies have used radio-labeled isoDGR dimer peptide to detect integrin $\alpha 5\beta 1$ -positive tumors (18), demonstrating good *in vivo* and *in vitro* properties, as well as ideal pharmacokinetic properties, and initial clinical translational research has been conducted (15). Therefore, the present study investigated whether these molecular probes detect degenerative disc diseases,

which may provide innovative methods and ideas for the pathogenesis and treatment of disc degenerative diseases, as well as to further expand the application of isoDGR.

In the present study, SPECT imaging of ^{99m}Tc -3PisoDGR2 in the IVD injury model demonstrated clear imaging of IVD 30 min after the injection of the imaging agent, indicating that ^{99m}Tc -3PRGD2 promptly binds with integrin $\alpha 5\beta 1$ receptors. The distribution of ^{99m}Tc -3PisoDGR2 at different time points showed that the expression of integrin $\alpha 5\beta 1$ was induced after the establishment of the acute disc herniation model. With the progression of time, the uptake of imaging agents in the IVD showed an increasing tendency, reaching a peak 1 week postinjury and then gradually decreasing. Nevertheless, the imaging agent content remained at a high level until 2 months postinjury. The expression of integrin $\alpha 5\beta 1$ receptor in IVD was analyzed using IHC, and the results agreed with the uptake trend, which may be attributed to the molecular mechanism during the degeneration of IVD.

The high expression of integrin $\alpha 5\beta 1$ during the acute stage after disc injury plays a key role in initiating the downstream signal cascade amplification effect. After the integrin molecules bind to fibronectin fragments in the extracellular matrix, the allosteric activation of integrin is initiated to regulate focal adhesion maturation, remodel the actin cytoskeleton, and mediate “outside-in” signal transduction. Moreover, fibronectin fragment signals serve to activate the intracellular components and initiate “inside-out” signal transduction, thereby inducing upregulation of integrin in the vicinity of the focal adhesions, facilitating more effective sensing of changes in the cell-matrix and coordinating signal transduction. Such an underlying mechanism provides the possibility for clinical practice, i.e., the expression of integrin $\alpha 5\beta 1$ receptor can be quantitatively analyzed by non-invasive examination to help with the

evaluation of the stage of disc degeneration and the effect of clinical intervention.

The present study had several limitations. First, degeneration of the IVD is caused by a variety of complex factors, such as heredity, traumatic injury, and overloading stress. Second, the animal model established in this experiment only simulated acute disc herniation with AF damage after traumatic injury. Although the model has many similarities with human disc herniation regarding clinical manifestations, pathology, and immunology, it does not precisely simulate the chronic progression of IVDs in the human body. Third, patients with severe degeneration of IVDs are commonly observed in clinical practice; their IVDs have been severely degraded, and their NP may have atrophied and disappeared. It is unknown whether the same conclusion can be made regarding these patients. Thus, further studies are needed for more precise validation. Finally, integrin $\alpha 5\beta 1$ is not a cost-effective method for asymptomatic or slightly symptomatic patients who can easily be followed-up with MRI, which is less expensive and easier to perform.

CONCLUSIONS

In the present study, a novel radioactive molecular probe, called ^{99m}Tc -3PRGD2, was used for the first time in an animal model of acute disc herniation to preliminarily evaluate its diagnostic value in acute disc herniation. Through real-time observation *in vivo*, the use of ^{99m}Tc -3PRGD2 well reflected the expression pattern of integrin $\alpha 5\beta 1$ in acute disc herniation. As acute disc herniation progressed, the uptake of ^{99m}Tc -3PRGD2 reached a peak at 1 week postinjury. Our data established a correlation between the uptake of ^{99m}Tc -3PRGD2 in acute disc herniation and the

expression of integrin $\alpha 5\beta 1$, providing a solid theoretical basis for understanding the pathophysiology of acute disc herniation, developing a novel drug treatment, and providing a more precise clinical monitoring of the curative effects.

DATA AVAILABILITY STATEMENT

Reasonable requests to the available datasets should be directed to the corresponding author(s).

ETHICS STATEMENT

The animal study was reviewed and approved by Xuanwu Hospital. Written informed consent was obtained from the owners for the participation of their animals in this study.

AUTHOR CONTRIBUTIONS

JG: writing—original and draft data curation. CY: writing—review and editing. XT: animal support. LC: software. HG: methodology. QY: software and draft data curation. XW: language editing. HW and ZC: resources. FJ: writing—review and editing and project administration. All authors contributed to the article and approved the submitted version.

FUNDING

This study was supported by Beijing Municipal Science and Technology Commission (Grant number: Z191199996619048) and Beijing Municipal Commission of Education (Grant numbers: KZ202010025043 and 1192070315).

REFERENCES

- Vialle LR, Vialle EN, Suarez Henao JE, Giraldo G. Lumbar disc herniation. *Rev Bras Ortop.* (2010) 45:17–22. doi: 10.1590/S0102-36162010000100004
- Long DM, BenDebba M, Torgerson WS, Boyd RJ, Dawson EG, Hardy RW, et al. Persistent back pain and sciatica in the United States: patient characteristics. *J Spinal Disord.* (1996) 9:40–58. doi: 10.1097/00002517-199602000-00007
- Garrido E. Lumbar disc herniation in the pediatric patient. *Neurosurg Clin N Am.* (1993) 4:149–52. doi: 10.1016/S1042-3680(18)30616-8
- Mayer HM, Mellerowicz H, Dihlmann SW. Endoscopic discectomy in pediatric and juvenile lumbar disc herniations. *J Pediatr Orthop B.* (1996) 5:39–43. doi: 10.1097/01202412-199605010-00008
- Suthar P, Patel R, Mehta C, Patel N. MRI evaluation of lumbar disc degenerative disease. *J Clin Diagn Res.* (2015) 9:TC04–9. doi: 10.7860/JCDR/2015/11927.5761
- Kim JH, van Rijn RM, van Tulder MW, Koes BW, de Boer MR, Ginai AZ, et al. Diagnostic accuracy of diagnostic imaging for lumbar disc herniation in adults with low back pain or sciatica is unknown; a systematic review. *Chiropr Man Therap.* (2018) 26:37. doi: 10.1186/s12998-018-0207-x
- Khan AN, Jacobsen HE, Khan J, Filippi CG, Levine M, Lehman RA Jr, et al. Inflammatory biomarkers of low back pain and disc degeneration: a review. *Ann N Y Acad Sci.* (2017) 1410:68–84. doi: 10.1111/nyas.13551
- Naqvi SM, Buckley CT. Extracellular matrix production by nucleus pulposus and bone marrow stem cells in response to altered oxygen and glucose microenvironments. *J Anat.* (2015) 227:757–66. doi: 10.1111/joa.12305
- Erwin WM, Hood KE. The cellular and molecular biology of the intervertebral disc: a clinician's primer. *J Can Chiropr Assoc.* (2014) 58:246–57.
- Nerlich AG, Bachmeier BE, Boos N. Expression of fibronectin and TGF-beta1 mRNA and protein suggest altered regulation of extracellular matrix in degenerated disc tissue. *Eur Spine J.* (2005) 14:17–26. doi: 10.1007/s00586-004-0745-x
- Yonezawa I, Kato K, Yagita H, Yamauchi Y, Okumura K. VLA-5-mediated interaction with fibronectin induces cytokine production by human chondrocytes. *Biochem Biophys Res Commun.* (1996) 219:261–5. doi: 10.1006/bbrc.1996.0215
- Pysz MA, Gambhir SS, Willmann JK. Molecular imaging: current status and emerging strategies. *Clin Radiol.* (2010) 65:500–16. doi: 10.1016/j.crad.2010.03.011
- Lindner JR, Link J. Molecular imaging in drug discovery and development. *Circ Cardiovasc Imaging.* (2018) 11:e005355. doi: 10.1161/CIRCIMAGING.117.005355
- Sun X, Li Y, Liu T, Li Z, Zhang X, Chen X. Peptide-based imaging agents for cancer detection. *Adv Drug Deliv Rev.* (2017) 110–1:38–51. doi: 10.1016/j.addr.2016.06.007
- Zhao H, Gao H, Zhai L, Liu X, Jia B, Shi J, et al. (^{99m}Tc) -HisoDGR as a potential SPECT probe for orthotopic glioma detection via targeting of integrin $\alpha 5\beta 1$. *Bioconjug Chem.* (2016) 27:1259–66. doi: 10.1021/acs.bioconjchem.6b00098
- Notni J, Steiger K, Hoffmann F, Reich D, Kapp TG, Rechenmacher F, et al. Complementary, selective PET imaging of integrin subtypes $\alpha 5\beta 1$ and

- alphavbeta3 using 68Ga-aquibepin and 68Ga-avebetrin. *J Nucl Med.* (2016) 57:460–6. doi: 10.2967/jnumed.115.165720
17. Notni J, Gassert FT, Steiger K, Sommer P, Weichert W, Rummeny EJ, et al. *In vivo* imaging of early stages of rheumatoid arthritis by alpha5beta1-integrin-targeted positron emission tomography. *EJNMMI Res.* (2019) 9:87. doi: 10.1186/s13550-019-0541-6
 18. Gao H, Luo C, Yang G, Du S, Li X, Zhao H, et al. Improved *in vivo* targeting capability and pharmacokinetics of (99m)Tc-labeled isoDGR by dimerization and albumin-binding for glioma imaging. *Bioconjug Chem.* (2019) 30:2038–48. doi: 10.1021/acs.bioconjchem.9b00323
 19. Zhang H, La Marca F, Hollister SJ, Goldstein SA, Lin CY. Developing consistently reproducible intervertebral disc degeneration at rat caudal spine by using needle puncture. *J Neurosurg Spine.* (2009) 10:522–30. doi: 10.3171/2009.2.SPINE08925
 20. Luo Q, Yang G, Gao H, Wang Y, Luo C, Ma X, et al. An integrin alpha 6-targeted radiotracer with improved receptor binding affinity and tumor uptake. *Bioconjug Chem.* (2020) 31:1510–21. doi: 10.1021/acs.bioconjchem.0c00170
 21. Fan D, Wang K, Gao H, Luo Q, Wang X, Li X, et al. A (64) Cu-porphyrin-based dual-modal molecular probe with integrin alphav beta3 targeting function for tumour imaging. *J Labelled Comp Radiopharm.* (2020) 63:212–21. doi: 10.1002/jlcr.3833
 22. Hoy D, March L, Brooks P, Blyth F, Woolf A, Bain C, et al. The global burden of low back pain: estimates from the Global Burden of Disease 2010 study. *Ann Rheum Dis.* (2014) 73:968–74. doi: 10.1136/annrheumdis-2013-204428
 23. Buchbinder R, van Tulder M, Öberg B, Costa LM, Woolf A, Schoene M, et al. Low back pain: a call for action. *Lancet.* (2018) 391:2384–8. doi: 10.1016/S0140-6736(18)30488-4
 24. Lee JH, Choi KH, Kang S, Kim DH, Kim DH, Kim BR, et al. Nonsurgical treatments for patients with radicular pain from lumbosacral disc herniation. *Spine J.* (2019) 19:1478–89. doi: 10.1016/j.spinee.2019.06.004
 25. Juniper M, Le TK, Mladi D. The epidemiology, economic burden, and pharmacological treatment of chronic low back pain in France, Germany, Italy, Spain and the UK: a literature-based review. *Expert Opin Pharmacother.* (2009) 10:2581–92. doi: 10.1517/14656560903304063
 26. Clark EA, Brugge JS. Integrins and signal transduction pathways: the road taken. *Science.* (1995) 268:233–9. doi: 10.1126/science.7716514
 27. Malik RK. Regulation of apoptosis by integrin receptors. *J Pediatr Hematol Oncol.* (1997) 19:541–5. doi: 10.1097/00043426-199711000-00013
 28. Li Y, Xu L, Olsen BR. Lessons from genetic forms of osteoarthritis for the pathogenesis of the disease. *Osteoarthritis Cartilage.* (2007) 15:1101–5. doi: 10.1016/j.joca.2007.04.013
 29. Forsyth CB, Pulai J, Loeser RF. Fibronectin fragments and blocking antibodies to alpha2beta1 and alpha5beta1 integrins stimulate mitogen-activated protein kinase signaling and increase collagenase 3 (matrix metalloproteinase 13) production by human articular chondrocytes. *Arthritis Rheum.* (2002) 46:2368–76. doi: 10.1002/art.10502
 30. Le Maitre CL, Frain J, Millward-Sadler J, Fotheringham AP, Freemont AJ, Hoyland JA. Altered integrin mechanotransduction in human nucleus pulposus cells derived from degenerated discs. *Arthritis Rheum.* (2009) 60:460–9. doi: 10.1002/art.24248
 31. Aota Y, An HS, Homandberg G, Thonar EJ, Andersson GB, Pichika R, et al. Differential effects of fibronectin fragment on proteoglycan metabolism by intervertebral disc cells: a comparison with articular chondrocytes. *Spine.* (2005) 30:722–8. doi: 10.1097/01.brs.0000157417.59933.db
 32. Kurakawa T, Kakutani K, Morita Y, Kato Y, Yurube T, Hirata H, et al. Functional impact of integrin $\alpha 5\beta 1$ on the homeostasis of intervertebral discs: a study of mechanotransduction pathways using a novel dynamic loading organ culture system. *Spine J.* (2015) 15:417–26. doi: 10.1016/j.spinee.2014.12.143
 33. Xia M, Zhu Y. Fibronectin fragment activation of ERK increasing integrin $\alpha 5$ and $\beta 1$ subunit expression to degenerate nucleus pulposus cells. *J Orthop Res.* (2011) 29:556–61. doi: 10.1002/jor.21273
 34. Zhang K, Ding W, Sun W, Sun XJ, Xie YZ, Zhao CQ, et al. Beta1 integrin inhibits apoptosis induced by cyclic stretch in annulus fibrosus cells via ERK1/2 MAPK pathway. *Apoptosis.* (2016) 21:13–24. doi: 10.1007/s10495-015-1180-7
 35. Behr TM, Gotthardt M, Barth A, Béhé M. Imaging tumors with peptide-based radioligands. *Q J Nucl Med.* (2001) 45:189–200.

Conflict of Interest: The authors declare that the research was conducted in the absence of any commercial or financial relationships that could be construed as a potential conflict of interest.

Publisher's Note: All claims expressed in this article are solely those of the authors and do not necessarily represent those of their affiliated organizations, or those of the publisher, the editors and the reviewers. Any product that may be evaluated in this article, or claim that may be made by its manufacturer, is not guaranteed or endorsed by the publisher.

Copyright © 2022 Guan, Yuan, Tian, Cheng, Gao, Yao, Wang, Wu, Chen and Jian. This is an open-access article distributed under the terms of the Creative Commons Attribution License (CC BY). The use, distribution or reproduction in other forums is permitted, provided the original author(s) and the copyright owner(s) are credited and that the original publication in this journal is cited, in accordance with accepted academic practice. No use, distribution or reproduction is permitted which does not comply with these terms.